“Mircea cel Batran” Naval Academy Scientific Bulletin, Volume XVIII – 2015 – Issue 1
Published by “Mircea cel Batran” Naval Academy Press, Constanta, Romania // The journal is indexed in:
PROQUEST SciTech Journals, PROQUEST Engineering Journals, PROQUEST Illustrata: Technology, PROQUEST Technology Journals, PROQUEST Military Collection PROQUEST Advanced Technologies & Aerospace

EVALUATION OF STRESSES AND STRAINS DURING THE APPLICATION PROCESS FINPLAST

Dorin Andrei D. DASCALU[1]
Dumitru I. DASCALU[2]
[1] As. Drd. Arh. Architecture University “Ion Mincu”, Bucharest, ROMANIA, dascalu.dorin@yahoo.com
[2] Associate prof. PhD, “Mircea cel Batran” Naval Academy, Constanta, ROMANIA, dumitru_dascalu2005@yahoo.com

Abstract: *FINPLAST is an original method proposed for anti-friction surface finish of the sliding bearings. The process extends cold plastic deformation technology, for finishing antifriction surfaces of the sliding bearings. In this paper presents the results of the evaluation of the state of stresses and strains obtained by simulation using the finite element method.*
Key words: *FINPLAST, proceeding, finishing surfaces, antifriction, bearings.*

Introduction

The paper takes stock of the stresses and strains of anti-friction material layer of sliding bearings, which are generated during the finishing process by process FINPLAST. The proposed method is an original solution of finishing by cold plastic deformation layer of anti-friction bearings to slip.
These conditions stress and strain is a support to assess the effects of this on the layer characteristics obtained. The evaluation was conducted by numerical simulation. For the study opted for contact between a cylinder of diameter 25mm hardened steel and anti-friction coating material plan based on aluminum alloy, plated on a plate OL 37.
For the calculation started from the general equation form the finite element method:

$$[M]\{\ddot{u}\}+[C]\{\ddot{u}\}+[K]\{u\}=\{F\} \qquad (1)$$

in that established notations have been used:
- [M] -matrices consistent masses;
- [K] - stiffness matrix;
- [C] - damping matrix;
- {F} - column vector of external forces;
- {P} - column vector of external forces applied in knots;
- {F} - vector finite elements distributed on the surface forces;
- [B] - depreciation matrix constants.

Based on the characteristics of the aluminum-based antifriction studied it is necessary to use the corresponding constituent relationships. displacement and rotation is infinitesimal suppose, and linearity calculation is only due to the material behavior. For the numerical simulation model was chosen a plan in Figure 1. The simulation consisted of achieving the three sequences of real phenomenon. In the first sequence, enter the vertical roll material, to a depth of 0.12mM and calculated theoretical force simulation was 280,5daN.
Second sequence gives the time of roll themselves in witch the movement has been made with 1mm horizontal. Withdrawal vertically until contact tensions have become void, constituting the third sequence.

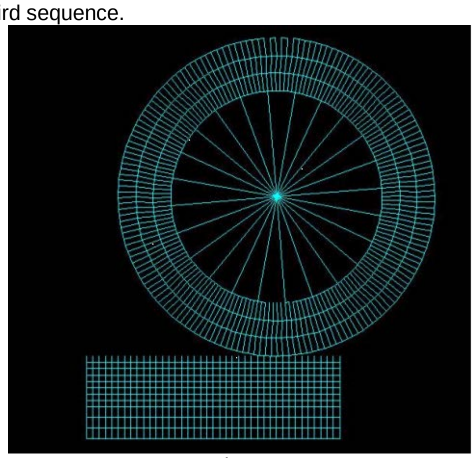

Fig.1

Meshing the model as illustrated in Figure 1. made for one roll, aluminum layer and backing plate 37 OL elements 2D plane type and to reduce the operating time remaining Trurs roller type 2D (spoke).
The method of integration was Newton-Raphson method.

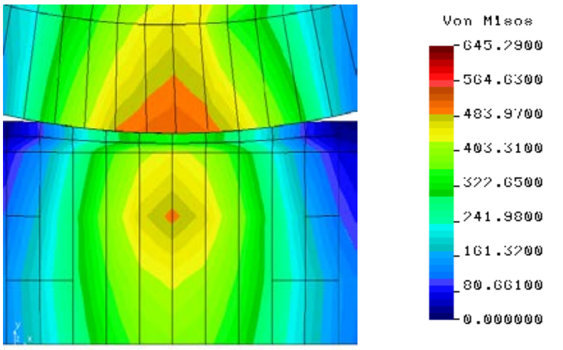

Fig.2. Starea de tensiuni efective σ (von misses) la sfârşitul primei secvenţe

The maximum number of contact points was 9 at the end of the first sequence and the second sequence number was 7. Step temporal was Δt = 0.005. It was considered a coefficient of friction μ = 0.2, for aluminum a σC = 40 N / mm^2, E = 0,69x105 N / mm^2 and G = 600 N / mm^2. Aluminum alloy layer of 0.4mm was considered and the support of the g = 2.5 mm OL37. Running programs was made using the program COSMOS / M, respectively: Geostar. For numerical simulation the program used generalized Hooke's law. According to energy theory (Von Mises) program calculates the total and the plastic deformations, the elastic yielding the difference. Using generalized Hooke's law program can offer us virtually tension state, in all directions, both actual (Von Mises) and the partial plan directions.
Determination and analysis of the state of tension in the finished layer by process FINPLAST

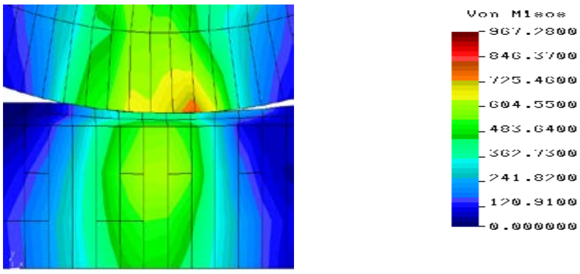

Fig. 3. Starea de tensiuni efective (von misses) în tipul secvenţei a–II-a

In figures 2, 3 and 4 is shown actual state of tension $\bar{\sigma}$ (Von Mises) corresponding to those 3 sequences. It is noted deformability properties of the anti-friction layer to make all three sequences appear in the layer of lower tensions than in the other two bodies.
From Figure 2. the stress is remarkable different from the three bodies due to their mechanical properties. For maximum tensions are rigid roll surface contact area, large deformations due to anti-friction layer tension properly distributed, making the shift toward

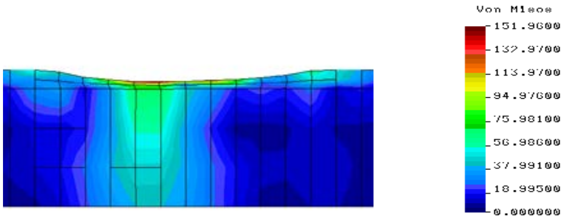

Fig. 4. Starea de tensiuni efective σ (von misses) secvenţa a-III-a, dupa retragerea rolei

support plate, the maximum values are at a certain depth, with a specific distribution of materials Elastoplast. Approximately square field tension maximum depth of the support plate, shows the depth at which the tension is null strains tensor. From Figure 3. actual state of tension that plays proper sequence II stands elastic properties of steel roller and support that make maximum stress areas to move more to the right, the contact geometry, visible especially in the roll. By contrast geometric means of the perpendicular intersection point corresponding lower roll center and the plane rolled surface area. Elastic characteristics of the support plate produce a mismatch state of stress and deformation, resulting in the disappearance of the equilibrium point of the first sequence. In this sequence is observed deformation wave formation in front of the roller in its sense of displacement, which generates a much larger contact area to the geometric contact to the remaining area after it. Because the layer of material resulting from cutting has a lower plasticity, because AIS (Chipping Layer Influenced by [1]) deformation creates great opportunities that make these tensions are lower than behind geometric contract where the elastic component deformation, especially of the support plate, roll and less anti-friction material layer produces a state of tension with higher values as shown in the figure. When driving roller distributes load (thanks wave and plastic deformation and elastic recovery of the support plate and anti-friction layer) over a length greater external values of effective tension, decreasing. Another interesting aspect is noted in the upper layer where due plasticity of material and resistance lower than the other buildings, the material deforms over tension remaining constant. Also due to difference different properties of materials in contact, tension between them show jumps. Valuable notes that the sequence II, maximum tensions in the layer antilimited contact with the support plate-400N / mm^2. The support plate values are limited to a maximum of ~ 600 N / mm^2. Deflection roller support plate in the direction of movement makes effective tensions to diminish greatly and while the tension is reduced in this scope. It is noted from the sequence I, the maximum displacement of the points of application as a result of the contact geometry, the maximum tension on the vertically moving arrive at the surface.

In figure 4 effective tension $\overline{\sigma}$ is shown after the roller withdrawal . As shown in this figure are greater tensions layer of anti-friction material layer than mass support plate. We believe that the main cause is the very low thickness of this layer (0.4 mm prior to deformation) and differences in mechanical properties, therefore different deformations occurring.

It is noteworthy that the same figure, the right contact geometric, only the top layer of steel plate remains tense, the rest due elatoplasticy anti-layer and the assembly of the support plate remains neutral. The highest values of $\overline{\sigma}$ remain in the area's last contact roller, slightly asymmetrical, moving geometric after contact. Also, withdrawal roller tension generated a real different from that given by the roll movement. From the point of view of tension values it is to note that the sequence II are reached maximum values of 967.78 N / mm^2 to 645.79 daN / mm^2 in the sequence I and 151 daN / mm^2 residual stress in the sequence III. Different mechanical properties of the two materials, resulting in all three figures, the change of state of tension to shift from anti-friction layer support board.

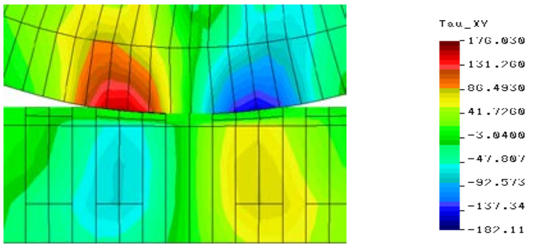

Fig. 5. Starea de tensiuni efective de forfecare (von misses) în tipul secvenþei a-III-a.

Figure 5. show effective tangential $\overline{\tau}_{xy}$ (Von Mises) in sequence II. It is worth mentioning here the effect of strain wave that due to large deformations induce both roller and anti-friction layer relatively high tensions $\overline{\tau}_{xy}$. In the central area, where the phenomenon occurs when the flow of material virtually shear stresses are much lower and relatively constant. It also noted that due to very good formability of aluminum tensions have very low values and nearly constant throughout the meal. The phenomenon of plastic flow in the vicinity of the contact area and geometrically in the other two bodies produce emergence of four areas where the state of shear stresses present specific configurations. Forming roller wave distortion and rigidity make these tensions to the maximum outside before contact roller and geometric and symmetrical negative values maximum close behind it.

As for the actual tension $\overline{\sigma}$, the anti-friction layer support plate assembly elastoplasticy generates the shearing stress state of the maximum positive and negative values at a certain depth in the support plate. This time in opposition to the state of stress $\overline{\sigma}$ in the oven, negative values are to the maximum contact geometric and positive and negative comparable values after this point. Zero values of these tensions appear on the contact line separating the two zones geometrically both roll and support plate.

Because different strains of residual plastic layer and anti-friction material support plate with much better elasticity and thickness greater separation in their area ~ tensions $\overline{\tau}_{xy}$ of 50-60 N / mm^2. Almost perfect geometric symmetry shows that at relatively small distances to the contact, finishing by plastic deformation influence is negligible. Further, it will analyze stress σ on the vertical and horizontal Ox Oy.

Vertical distribution σy tensions sequence is shown in Figure 6.

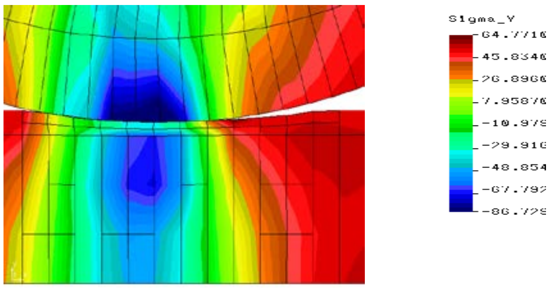

Fig.6. Starea de tensiuni σ_y, în timpul secvenţei a-IIa

The effect is remarkable wave distortion in the distribution of these stresses, deformations due to the relative sliding generating a jump in the distribution of these tensions between the roller and anti-friction layer. Also, as in the case of effective stresses $\overline{\sigma}$, due to the same reasons there is a shift to the right of the area of maximum demand. It is noted that due to the support plate tension higher values are anti-friction layer depth. Although anti-friction material thickness is very small, the phenomenon of plastic flow causes tensions vertical variations of it to be significant. The maximum reach ~500N / mm^2 and compression are tensions. Tensile stresses due to the elastic component, comprising areas are smaller value higher. Asymmetry is significant due to the wave of deformation in this case.As with the actual tensions, the maximum values are in the depth of the support plate, but near the contact surface tends to achieve and the layer of anti-friction material. In this case, local values are worth very large tension compression, reaching values of about 720N / mm^2 in the contact area of the roller and 680N / mm^2, the support plate and the separation of its anti-friction layer.

Of course, if the problem studied most interest presents residual tension σy state, the sequence shown in Figure 7 III. Homologous II, it presents differences. Different properties of the two materials of the assembly formed by the anti-friction layer and support plate, the elastic and plastic deformations of the two different components, generate compressive residual stress σ_y as well as tension. This is even more decisive in the transition area between the two materials. Regarding the anti-friction layer, it is noteworthy difference before contact state of tension and geometric behind him. It notes the existence of the right image, the top anti-friction layer, a layer ~ strong in compression with 65daN / mm^2 due to the elastic component of the central area of the support plate, the strongest deformed by contact geometric area of anti-friction material. It expands with the disappearance of the roller compression force. Section greater support plate, much better elasticity of steel generates a large elastic component, which makes the roll after the withdrawal, the maximum area to migrate to request anti-friction layer, the plastic component is dominant, reaching maximum values compression to the surface layer of the support plate and anti-friction material layer in the immediate vicinity. Extending σy residual stress analysis in Figure 7. the existence of compressive stress resulting from the maximum values of 86.77 N / mm^2 and tensile values of up to 64.77 N / mm^2. Areas, with the two

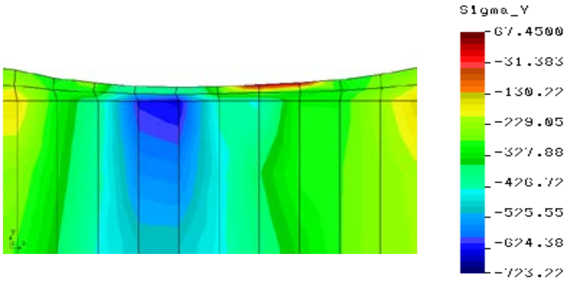

Fig.7. Starea de tensiuni remanente σ_y, secvenţei a-III-a

extreme values are shifted in the horizontal direction and vertical maximum compression as the support plate, the contact area geometry, where the second sequence has ended and the maximum tension at the surface of the anti-friction layer in the region of sequence I and II.

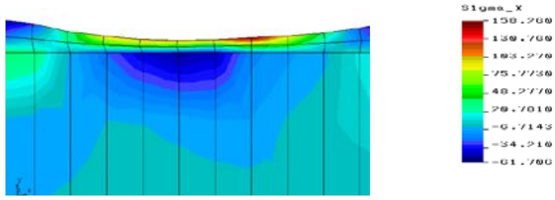

Fig.8. Starea de tensiuni σ_x după retragerea rolei

Roll retirement sequence before to end anti-friction layer, makes the existence of deformation wave symmetry to cancel σy residual tensions. Was observed to maintain the anti-friction layer of compressive stress in the support plate ~ 67 N / mm^2. For a more complete picture of the state of residual stress in Figure 8 σx tension state is shown, which gives details about the state of stress in the horizontal plane. And this figure shows that values much higher mass and elastic deformation of the board, compared with anti-friction layer, predominantly plastic deformations makes that request with the disappearance of the roller support plate to generate anti-friction layer tensions ~ stretch three times the compression of the support plate. In addition, layer shrinkage after the withdrawal roller (elastic component) at the beginning and end of the sequence makes anti-friction coating to supplement extent to values of 158 N / mm^2. It also notes two contradictory effects of the deformation wave that Ox direction generates a compression layer outer surface layer anti-friction and tension in the separation of anti-friction layer and the support plate. Training wave front deformation generates tensions between the layer of anti-friction roller and support plate with values of about 80 daN / mm^2. Due to the mechanical properties and different degrees of deformation of the two materials, their tendency to detachment may occur. In conclusion it is worth mentioning the existence of a complex stress state in the layer of antifriction material subject to cold plastic deformation, moving from the compression to the tension, which can lead to structural changes in solid state, the complex effects on the properties of the anti-layer material.

Bibliography

[1] Dascălu D. The phenomenon of pitting at the anti-friction alloys, Engineering Meridian, No.1. 2006, Chişinău,

[2] Dascălu D. Pre-configuring the optimal structure manufacturing antifriction bearing, Engineering Meridian Nr.1. 2006, Chişinău